Synthesis of dense bulk MgB_2 by an infiltration and growth process

A G Bhagurkar[1], A Yamamoto[2, 3], N Hari Babu[1], J H Durrell[4], A R Dennis[4], D A Cardwell[4]

[1]Brunel Centre for Advanced Solidification Technology, Brunel University, Uxbridge, UB8 3PH, UK

[2] Department of Superconductivity, University of Tokyo, 7-3-1 Hongo, Bunkyo-ku, Tokyo, 113-8656, Japan

[3]JST-PRESTO, 4-1-8 Honcho, Kawaguchi, Saitama 332-0012, Japan

[4]Bulk Superconductivity Group, Department of Engineering, University of Cambridge, Trumpington Street, CB2 1PZ, UK

Abstract: We report the processing of dense, superconducting MgB_2 ($\rho \approx 2.4$ g/cm^3) by an infiltration and growth technique. The process, which involves infiltration of liquid magnesium at 750 ºC into a pre-defined boron precursor pellet, is relatively simple, results in the formation of a hard, dense structure and has the potential to fabricate large bulk samples of complex geometries. X-ray diffraction has been used to confirm the presence of the MgB_2 primary phase with only residual magnesium content in the fully processed samples. The samples exhibit sharp superconducting transitions at 38.4 K and have critical current densities of up to 260 kA/cm^2 in self-field at 5 K. Modest measured values of $Hc_2(0)$ of 17 T suggest that superconductivity in bulk MgB_2 fabricated by this technique is in the clean pairing limit.

Introduction

Superconductivity in magnesium diboride (MgB_2) was discovered in 2001 [1]. The relatively high T_c (39 K), high critical current density, long coherence length (~6 nm) [2], low raw material cost, lower density and relative ease of fabrication make this material an exciting choice for practical applications. Furthermore, lower anisotropy and strongly linked current flow in untextured polycrystalline samples of bulk MgB_2 has enabled the development of different processing routes to fabricate MgB_2 in the form of wires, tapes, thin films and bulks [3,4].

All the superconductors discovered over the past thirty years, despite having higher transition temperatures and critical current densities, have been unable to replace Nb based superconductors in commercial applications due primarily to difficulties associated with processing. In HTS materials, for example, strong crystallographic texture is necessary since grain boundaries inhibit strongly the flow of inter-granular current [5]. This also limits the thickness of the tape or bulk form of material to which they can be made [6]. Given these limitations, MgB_2 could be a good choice of material for applications that operate around temperatures of around 20 K that are achievable using compact, cryo-coolers without the need for liquid helium. Unfortunately, the volatility of Mg during processing has hindered greatly its prospects for practical applications in the short term.

Conventionally, MgB_2 processed in the form of wires and tapes can be synthesized either by an *ex situ* or *in situ* sintering technique. Grasso *et al* have reported high J_c using the *ex situ* route without any thermal treatment [7], although the relatively poor self-sintering nature of MgB_2 grains results in weaker inter-grain coupling. As a result, overall connectivity is often poor in these samples, even for long sintering times [8]. Moreover, a higher reaction

temperature results in the decomposition of MgB_2 to form Mg and MgB_4 [9], which can further deteriorate the properties of the fully processed material. *In situ* synthesis from elemental (Mg+B) powder, on the other hand, is relatively simple and yields the MgB_2 phase after a sintering time as little as 2 hours [10]. However, this processing route often results in the formation of a highly porous structure (up to 50%) due primarily to the high vapour pressure of magnesium and 28% volume shrinkage associated with MgB_2 phase formation [11]. Precursor powders for the fabrication of bulk MgB_2 are therefore often enriched with Mg to compensate for lost Mg vapour during processing. Although this leads to improved grain connectivity, porosity is still unavoidable in the fully processed bulk [12], and weak links are created frequently by the formation of oxides such as BO_x and MgO, which reduce the effective current carrying cross sectional area of the sample [13, 14]. There have been numerous reports of the synthesis of bulk MgB_2 via sintering, and a number of studies have shown that high pressure and elevated temperature [15,16] are effective in promoting MgB_2 phase formation and subsequent sintering. The use of high-pressure leads typically to the introduction of defects in the MgB_2 structure that form effective pinning centres [17]. Although this approach results in a high critical current density, the need to use large pressure vessels represents a significant practical limitation for the development of a practical process and of the achievable dimensions in the final MgB_2 sample.

Several authors have adopted a low temperature, solid-solid reaction approach for the fabrication of MgB_2 to avoid vaporization of Mg during processing. Rogado *et al* first reported the *in situ* synthesis of MgB_2 at a temperature as low as 500 ºC [18]. Kumakura *et al* subsequently proposed a technique based on "internal Mg diffusion", which involved placing Mg rod along the axis of a B powder compact in a sealed tube, followed by cold working and then annealing at 600 ºC [19]. Similarly, Goldacker *et al* obtained high transport J_c in fine

grain MgB_2 fabricated *in situ* at low temperature (640 ºC) [20], which resulted in the formation of a highly dense MgB_2 phase. Yamamoto *et al* have proposed a "powder in closed tube" method that involves packing Mg and B powders densely in the form of tapes in a sealed tube by applying a high uniaxial pressure prior to sintering [21]. This method was found to be effective in confining the Mg vapour in the reaction chamber, which led to a high MgB_2 bulk density. The same process at lower reaction temperature (600 ºC) yielded a finer grain and a reduced crystalline MgB_2 phase content, both of which contributed to an increase in flux pinning force and J_c [22]. Alternatively, Togano proposed an "interface diffusion" method using layers of Fe-Mg alloy as source of Mg with a layer of B powder sandwiched between the layers and then annealed. Mg atoms were observed to diffuse into the B grains during this process to yield a dense MgB_2 tape containing relatively little porosity [23]. Finally, Fujii *et al* and Matsumoto *et al* used MgH_2 as a source of Mg. The H_2 produced following the decomposition of MgH_2 forms a reducing atmosphere, which results in reduced oxidation of Mg and the formation of a well-connected MgB_2 phase [24,25]. These improvised methods largely avoid the problem of Mg vaporization, resulting in the formation of a dense microstructure with high critical current densities. However, these techniques tend to be difficult to scale up to form bulk MgB_2 components for practical applications due to limited diffusion of Mg into B at low temperatures [26] and long reaction times associated with the process. As a result, the fabrication of high density, bulk MgB_2 remains a challenging processing problem.

Here, we report the synthesis of bulk MgB_2 by the infiltration of liquid Mg into porous B precursor. This process has been adapted from the "infiltration and growth" technique used to synthesize bulk Y-Ba-Cu-O (YBCO) superconductor, which involves infiltrating Ba-Cu-O liquid into solid Y_2BaCuO_5 (Y-211) followed by a controlled peretectic reaction to yield the

target superconducting $YBa_2Cu_3O_{7-\delta}$ (Y-123) phase [27,28]. The infiltration and growth process offers potentially significant advantages for the Mg-B system due to its lower reaction temperature and the inherent capability of MgB_2 fabricated in polycrystalline form to carry large current. This relatively simple method not only results in the formation of hard, dense structures but also has the potential to fabricate complex geometries, which are not achieved easily using conventional sintering techniques.

The infiltration route for processing MgB_2 fibers (of diameter 160 μm) was first reported by Canfield *et al* [10] and involves exposing B fibers to Mg vapour at 950 ºC. Later, Dunand *et al* [29] reported the synthesis of Mg-MgB_2 composites by infiltrating liquid Mg under pressure at 800 ºC into a B preform. Improved versions of this process were reported subsequently by Giunchi *et al* [30] for the fabrication of bulk MgB_2 artefacts, in which Mg bulk and B powder are placed in a metallic container. The container was then welded closed and heat-treated at 950 ºC to obtain dense, bulk MgB_2, with the initial arrangement of B and Mg bulk in the container being used to define the geometry of the final product [31].

Experimental

Disc shaped precursor bodies (20 mm diameter and 4 mm thickness) were prepared from 99.99% (44 μm) purity amorphous boron powder (Alfa Aesar) under an applied uniaxial load of 5 MPa. The green density of the precursor pellet was engineered to be around 40% of the theoretical value, so that any residual pores in the bulk microstructure could be infiltrated by liquid Mg during processing to satisfy the overall compositional stoichiometry. A boron pellet was sandwiched initially between Mg blocks of commercial purity, as shown in Fig. 1(a). The magnesium was then melted at 750 ºC in a graphite crucible for 2 hours. Excess liquid Mg was used in this process in view of its high vapour pressure and to maintain a

positive fluid pressure aid to infiltration. A N_2 + SF_6 (95:5) cover gas mixture was maintained to minimize the oxidation of Mg during the process. The excess Mg was removed from the sample by machining after cooling to room temperature and the MgB_2 disc recovered, as shown in Fig 1(b). Several small specimens of size 3 mm*3 mm*1 mm were cut from the MgB_2 bulk for further characterization. The density was determined from simple mass and volume measurements to be 90% of the theoretical density. The microstructure and fracture surface of the infiltrated sample was examined by scanning electron microscopy (SEM), and X-ray diffraction (XRD) was performed to analyse the phase content of the sample. The magnetic moment of sample was measured using a superconducting quantum interference device (SQUID) magnetometer. Critical current density was calculated from the measured magnetic moment loop using the extended Bean model for a rectangular cross section in a perpendicular magnetic field [32]. Finally, a four-probe resistance technique was used to measure the resistivity of the sample under an applied external field of up to 9 T (applied perpendicular to the direction of transport current).

Results and Discussion

Figure 2 shows an X-ray diffraction powder pattern for the MgB_2 sample fabricated by infiltration and growth, which confirms that the specimen consists of a majority MgB_2 phase with residual MgO and Mg. The presence of Mg is commonly observed in infiltration studies [29, 30] and associated with the dense packing of the MgB_2 unit cell, which creates voids that become occupied by surrounding liquid Mg during processing. Detailed analysis suggests that material has about 5% MgO and13% Mg. MgO has likely formed as a result of reaction between excess Mg and O during milling process that was used to powder the bulk. Giunchi *et al* reported the presence of boron rich phases such as $Mg_2B_{25,}$ MgB_4 or MgB_7 in the reactive liquid infiltration process [31,33], although no such phases were detected in the

samples prepared in this study. This may be explained by the Mg-rich atmosphere generated intrinsically as part of the fabrication process, which facilitates the formation of Mg-rich borides in the MgB_x family, and MgB_2 in particular.

Figure 3(a) shows a secondary electron image of the fracture surface of the MgB_2 bulk sample, which reveals a dense microstructure and clean grain boundaries. Significantly, no impurities or porosity are observed in this image. A higher magnification micrograph of the same fracture surface is shown in Fig 3(b), from which the presence of hexagonal plate-like crystals can be observed. This is due primarily to the rapid crystal growth parallel to the *a-b* plane; such geometry is typical of hcp borides that exhibit faceted growth. The grain size can be estimated from this micrograph to be around 500 nm. A similar morphology has been reported previously for MgB_2 [34]. Giunchi *et al* also observed the presence of several grains of size 100 μm after processing at 950 ºC in a similar experiment [30], suggesting that such fine grain size is due potentially to the use of a lower reaction temperature (750 ºC), which limits grain growth. Such homogeneous microstructure is attributed presence of excess Mg during reaction, which is known for improving grain connectivity, elimination of micro-cracks, facilitating recrystallization and avoiding B-rich impurities [35].

The normalised field cooled (FC) and zero field cooled (ZFC) magnetic moment for the bulk MgB_2 fabricated by infiltration and growth are shown in Fig. 4 for an applied field of 1 mT. A sharp superconducting transition at 38.4 K and transition width of 0.7 K is observed in both sets of data, which suggest that bulk sample prepared in this study is homogeneous.

Fig. 5 shows the variation of critical current density, J_c, as a function of applied field at 5 K, 20 K and 30 K. J_c at 5 K and 20 K under self-field is as high as 260 kA/cm^2 and 200 kA/cm^2,

respectively, suggesting that the sample is well connected with a relatively large current carrying cross sectional area. J_c decreases appreciably in higher applied field, which is indicative of weak flux pinning in this field regime. Giunchi *et al* obtained slightly high J_c of 80 kA/cm^2 (20K, 2 T) with RLI process [36]. Similarly Maeda *et al* (10^3 A/cm^{2,} 20 K, 4T) [37], Yamamoto *et al* (600 kA/cm^2, self-field 20 K) [11] reported high J_c in ambient pressure in-situ sintering route. Prikhna *et al* recently reported very high J_c of 900 kA/cm^2 (Self field, 20 K) using high pressure [38]. Obtained J_c here, although modest when compared to these data, is relatively high taking into account residual Mg content.

Figure 6 shows the variation of resistivity with temperature for the MgB_2 bulk sample between 300 K and 5 K in an applied external field up to 9 T. For a comparison, normalised ZFC magnetic transition is also plotted (Figure 6 inset). Although T_c offset is slightly reduced (difference of .4 K) in inductive mode, T_c onset is quite close (difference is ≈.02 K). Such behaviour has previously been observed and is attributed to the transport current path in resistive measurement that chooses good quality grains (least resistance) [39]. This is in contrast to the inductive measurement where current loop passes through surface of material which includes good and poor quality grains. The observed low difference in measured T_c by two separate techniques suggests that the material is indeed homogeneous.

The sample exhibits a very low residual resistivity of 2.64 μΩcm and a residual resistivity ratio (RRR) of 5.63, which is comparable to values observed for single crystal MgB_2 samples (typically 1-2 μΩcm measured in-plane), as reported previously [2,40,41]. In addition, the observed increase in resistivity with external field at a given temperature indicates that the bulk MgB_2 sample exhibits significant magneto resistive effects. The normal state electrical connectivity (K) (or effective cross sectional area), which is defined by Rowell [9] as the

ratio of difference of resistivity between a single crystal to that of a polycrystal, is calculated for the MgB_2 bulk sample from the following expression:

$$K = \frac{\rho sc(300\ \mathrm{K}) - \rho sc(40\ \mathrm{K})}{\rho(300\ \mathrm{K}) - \rho(40\ \mathrm{K})} = 51.8\% \qquad \begin{matrix} \rho sc(300\ \mathrm{K}) - \rho sc(40\ \mathrm{K}) = 6.32\ \mu\Omega\mathrm{cm} \\ \rho(300\ \mathrm{K}) - \rho(40\ \mathrm{K}) = 12.2\ \mu\Omega\mathrm{cm} \end{matrix}$$

where ρ_{sc} is the resistivity of an MgB_2 single crystal averaged over random orientations and ρ is the resistivity of MgB_2 fabricated by infiltration and growth. Difference of resistivity of single crystal between 300 K and 40 K (ρ(300 K)- ρ(40 K)) is taken as 6.32 μΩcm based on predictions of mean field theory in [11]. The connectivity obtained here is significantly higher than that observed in bulk MgB_2 samples synthesized by both *ex situ* (~10%) and *in situ* (~30%) ambient pressure processing routes [8].

It is important to note that the transport properties of the present sample are altered by residual magnesium metal within the infiltrated grown sample. ρ-T plot for pure MgB_2 shows plateau near 80 K, whereas ρ-T curve for Mg exhibits linear decrease till 40 K [42]. Magneto-resistance is another evidence for the contribution of residual magnesium on current transport [43]. It is evident from figure 6 that ρ-T curve obtained here has characteristics of MgB_2 as well as Mg. Thus it is likely that ρ(300 K) and ρ(40 K) are underestimated whereas RRR and connectivity are overestimated in the present case. A prediction of connectivity in such case would require numerous samples with known amount of excess Mg. The intercept of extrapolated ρ(T) *versus* excess Mg curves would yield a fairly good value of ρ(300 K) and ρ(40 K) excluding any effects by Mg. These values can then be used to estimate corrected value of connectivity.

Figure 7 shows the variation of upper critical field, H_{c2}, and irreversibility field, H_{irr}, with temperature, both of which have been estimated using the 90%-10% definition of the resistive transition. It can be seen that both H_{c2} and H_{irr} vary linearly at temperatures below around 34

K (i.e. slightly below T_c). A simple extrapolation of the curve yields a value of H_{c2} at 0 K of 17 T. This is rather lower than that obtained for polycrystalline MgB_2 [16] and is close to the value of Hc_2 for a single crystal (15 T in the *a-b* plane) [44]. This suggests that sample fabricated in the present study is transformed fully into highly crystalline MgB_2.

Conclusion

We have demonstrated the fabrication of dense and highly connected bulk MgB_2 by an infiltration and growth process. This relatively simple technique is performed at ambient pressure and is therefore potentially scalable to the fabrication of larger bulk MgB_2 samples of more complex geometries. X-Ray diffraction has revealed that MgB_2 is present in the bulk samples as the main phase with Mg and MgO present in minor quantities. Densification mechanism in this study differs significantly from conventional solid state sintering of MgB_2, in which the porosity is typically retained during processing resulting in poorly connected grains. J_c of the bulk MgB_2 samples in self-field is 200 kA/cm^2 (at 20 K) and is relatively high considering high residual Mg content. The good microstructural and superconducting properties of bulk MgB_2 fabricated by the infiltration and growth process are attributed to the presence of dense, fine grains and a pore free MgB_2 bulk microstructure. Finally, an upper critical field of 17 T has been observed for this sample, which is close to single crystal value and which indicates that bulk material is operating in the clean pairing limit for superconductivity.

Acknowledgements

The authors acknowledge financial support from the KACST-Cambridge Research Centre, Cambridge, UK. This work was partially supported by the Japan Science and Technology Agency, PRESTO.

References

[1] Nagamatsu J, Nakagawa N, Muranaka T, Zenitani Y and Akimitsu J 2001 *Nature* **410** 63

[2] Xu M, Kitazawa H, Takano Y, Ye J, Nishida K, Abe H, Matsushita A, Tsujii N and Kido G 2001 *Appl. Phys. Lett.* **79** 2779

[3] Kambara M, HariBabu N, Sadki E S, Cooper J R, Minami H, Cardwell D A, Campbell A M and Inoue I H 2001 *Supercond. Sci. Technol.* **14** L5–L7

[4**]** Larbalestier D C *et al Nature* **410** 186

[5] Dimos D, Chaudhari P, Mannhart J and LeGoues F K 1988 *Phys. Rev. Lett.* **61** 219

[6] Foltyn S R, Jia Q X, Arendt P N, Kinder L, Fan Y and Smith J F 1999 *Appl. Phys. Lett.* **75** 3692

[7] Grasso G, Malagoli A, Ferdeghini C, Roncallo S, Braccini V, Siri A S and Cimberle M R 2001 *Appl. Phys. Lett.* **79** 230

[8] Yamamoto A, Tanaka H, Shimoyama J, Ogino H, Kishio K and Matsushita T 2012 *Japanese J. of Appl. Phys.* **51** 010105

[9] Fan Z Y, Hinks D G, Newman N and Rowell J M 2001 *Appl. Phys. Lett.***79** 87

[10] Canfield P C, Finnemore D K, Bud'ko S L, Ostenson J E, Lapertot G, Cunningham C E and Petrovic C 2001 *Phys. Rev. Lett.* **86** 2423

[11] Yamamoto A, Shimoyama J, Kishio K and Matsushita T 2007 *Supercond. Sci. Technol.* **20** 658

[12] Zeng R, Lu L, Wang J L, Horvat J, Li W X, Shi D Q, Dou S X, Tomsic M and Rindfleisch M 2007 *Supercond. Sci. Technol.* **20** L43

[13] Rowell J M 2003 *Supercond. Sci. Technol*. **16** R17

[14] Klie R F, Idrobo J C, Browning N D, Regan K A, Rogado N S and Cava R J 2001 *Appl. Phys. Lett.* **79** 1837

[15] Takano Y, Takeya H, Fujii H, Kumakura H and Hatano T 2001 *Appl. Phys. Lett.* **78** 2914

[16] Jung C U, Park M, Kang W N, Kim M, Kim K H P, Lee S Y and Lee S 2001 *Appl. Phys. Lett.* **78** 4157

[17] Liao X Z, Serquis A, Zhu Y T, Civale L, Hammon D L, Peterson D E, Mueller F M,

Nesterenko V F and Gu Y 2003 *Supercond. Sci. Technol.* **16** 799

[18] Rogado N, Hayward M A, Regan K A, Wang Y, Ong N P, Zandbergen H W, Rowell J M and Cava R J 2002 *J. of Appl. Phys.* **91** 274

[19] Hur J M, Togano K, Matsumoto A, Kumakura H, Wada H and Kimura K *Supercond. Sci. Technol.* **21** 032001

[20] Goldacker W, Schlachter S I, Obst B, Liu B, Reiner J and Zimmer S 2004 *Supercond. Sci. Technol.* **17** S363

[21] Yamamoto A, Shimoyama J, Ueda S,Katsura Y, Horii S and Kishio K 2004 *Supercond. Sci. Technol.* **17** 921

[22] Yamamoto A, Shimoyama J, Ueda S, Katsura Y, Iwayama I, Horii S and Kishio K 2006 *Physica C* **445** 806

[23] Togano K,Nakane T, Fujii H, Takeya H and Kumakura H 2006 *Supercond. Sci. Technol*. **19** L17

[24] Fujii H, Togano K and Kumakura H 2002 *Supercond. Sci. Technol.* **15** 1571

[25] Matsumoto A, Kumakura H, Kitaguchi H and H Hatakeyama 2003 *Supercond. Sci. Technol.* **16** 926

[26] Kumakura H 2012 *J. Phys. Soc. Jpn*. **81** 011010

[27] N. Hari Babu, M. Kambara, P.J. Smith, D.A. Cardwell, and Y. 2000 *J. Mater. Res.* **15** 1235

[28] Sudhakar Reddy E, Noudem J G, Tarka M and Schmitz G J 2000 *Supercond. Sci. Technol.* **13** 716

[29] Dunand D C 2001 *Appl. Phys. Lett.* **79** 4186

[30] Giunchi G 2003 *Inter. J. of Modern Phys. B* **17** 453

[31] Giunchi G, Ripamonti G, Cavallin T, Bassani E 2006 *Cryogenics* **46** 237

[32] Chen D X and Goldfarb R B 1989 *J. Appl. Phys.***66** 2489

[33] Giunchi G, Malpezzi L, Masciocchi N 2006 *Solid State Sciences* **8** 1202

[34] Xi X X 2002 *Nature Materials* **1** 1

[35] Serquis A, Civale L, Hammon D L, Liao X Z, Coulter J Y, Zhu Y T, Peterson D E, and Mueller F M 2003 *J. Appl. Phys.* **94** 4024

[36] Giunchi G, Albsetti A F, Malpezzi L, Sagletti L and Perini E 2011 *Proceedings of 2011*

IEEE International Conference on Applied Superconductivity and Electromagnetic Devices 313

[37] Maeda M, Zhao Y, Nakayama Y, Kawakami T, Kobayashi H and Kubota Y 2008 *Supercond. Sci. Technol.* **21** 032004

[38] Prikhna T A, Eisterer M, Weber H W, Hawalek W, kovylaev V V, Karpets M V, Basyuk T V and Moshchil V E 2014 *Supercond. Sci. Technol.* **27** 044013

[39] Kulich M, Kovac P Eisterer M, Husek I, Melisek T, Weber H W and Hassler W 2009 *Physica C* **469** 827

[40] Eltsev Y, Lee S, Nakao K, Chikumoto N, Tajima S, Koshizuka N and Murakami M 2002 *Phys. Rev. B* **65** 140501

[41] Sologubenko A V, Jun J, Kazakov S M, Karpinski J and Ott H R 2002 *Phys. Rev.* B **66** 014504

[42] Kovac P, kulich M, Haessler W, Hermann M, Melisek T and Reissner M 2012 *Physica C* **477** 20

[43] Jung C U, Kim H J, park M S, Kim M S, Kim J Y, Du Z, Lee S I, Kim K H, Betts J B, Jaime M, Lacerda A H and G S Boebinger 2002 *Physica C* **377** 21

[44] Zehetmayer M, Eisterer M, Jun J, Kazakov S M, Karpinski J, Wisniewski A and Weber H W 2002 *Phys. Rev. B* **66** 052505

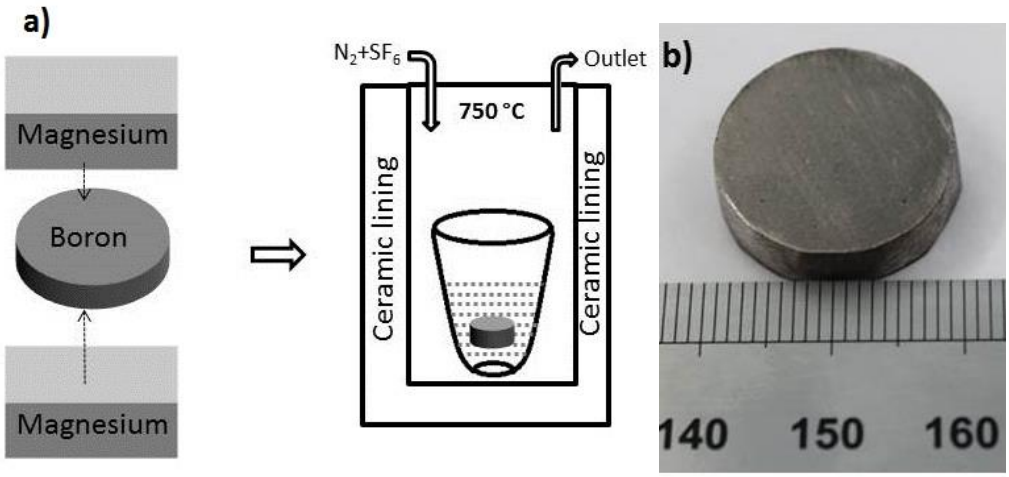

Fig 1 (a) Schematic of the infiltration and growth process and (b) Photograph of a MgB_2 disc fabricated by infiltrated and growth

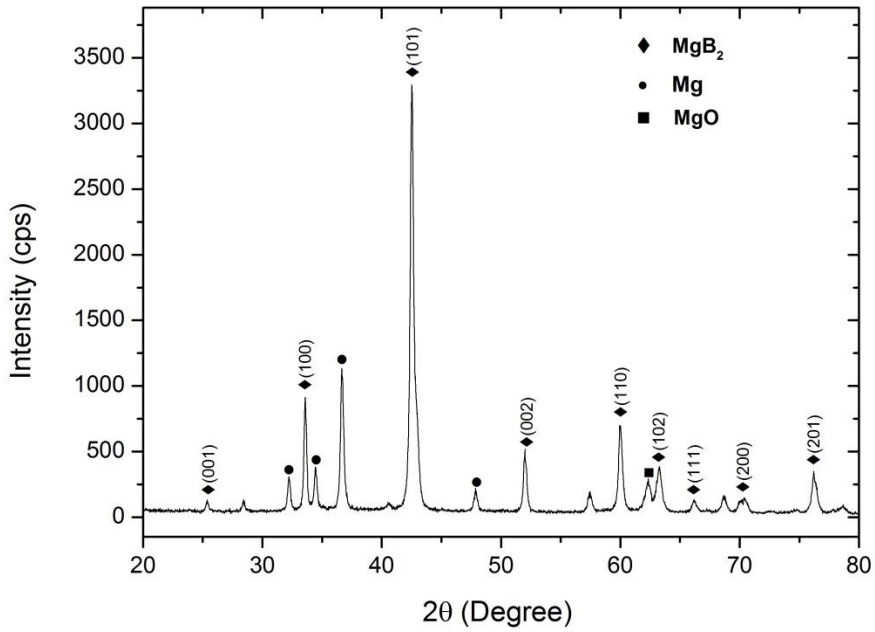

Fig. 2. X ray diffraction pattern of a MgB_2 powder specimen fabricated by infiltration and growth indicating the presence of Mg and MgO impurities. All MgB_2 peak positions are indexed.

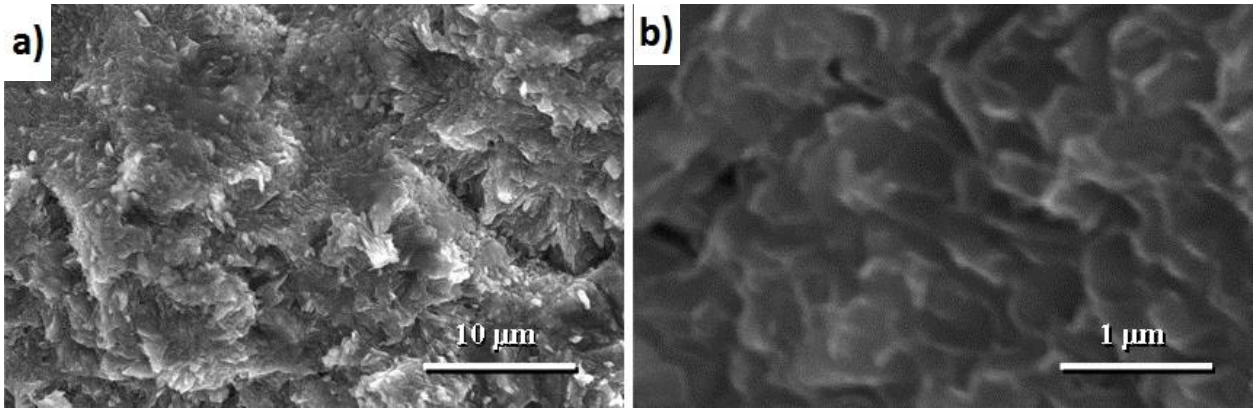

Fig. 3(a) SEM observation of the fractured bulk MgB_2 surface (b) fine grain structure

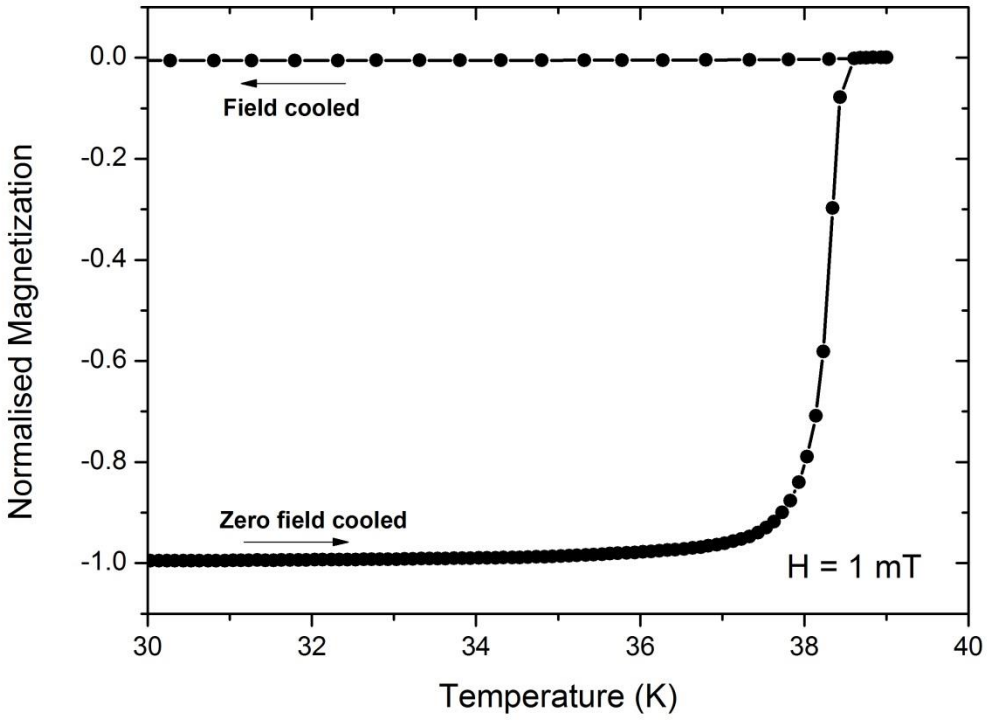

Fig. 4. Normalised magnetization of MgB_2 as a function of temperature, measured under zero field and field cooled conditions at 1 mT.

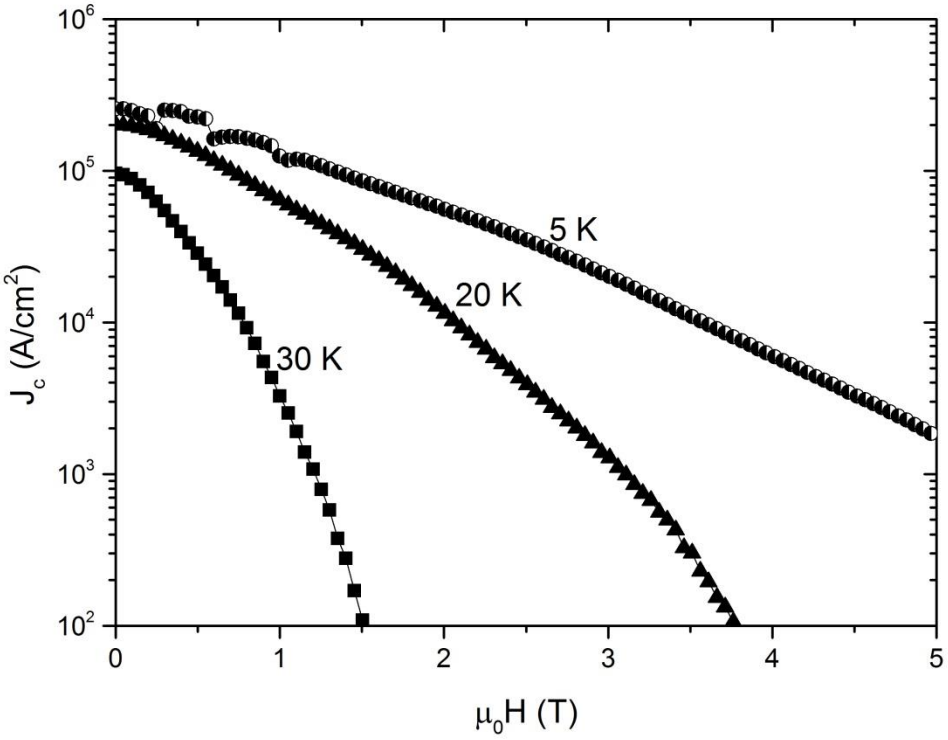

Fig. 5. Critical current density of bulk MgB_2 as a function of applied magnetic field

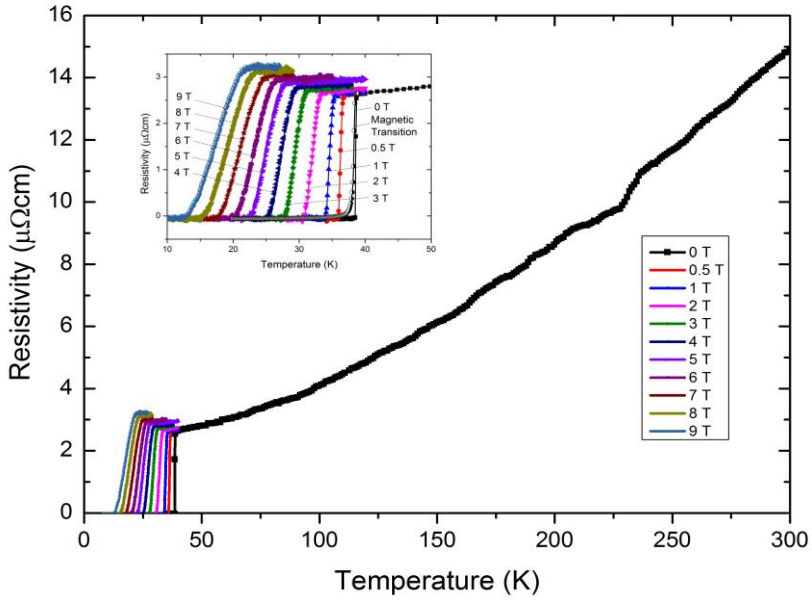

Fig. 6. Variation of the bulk MgB_2 resistivity with temperature at applied magnetic fields of up to 9 T

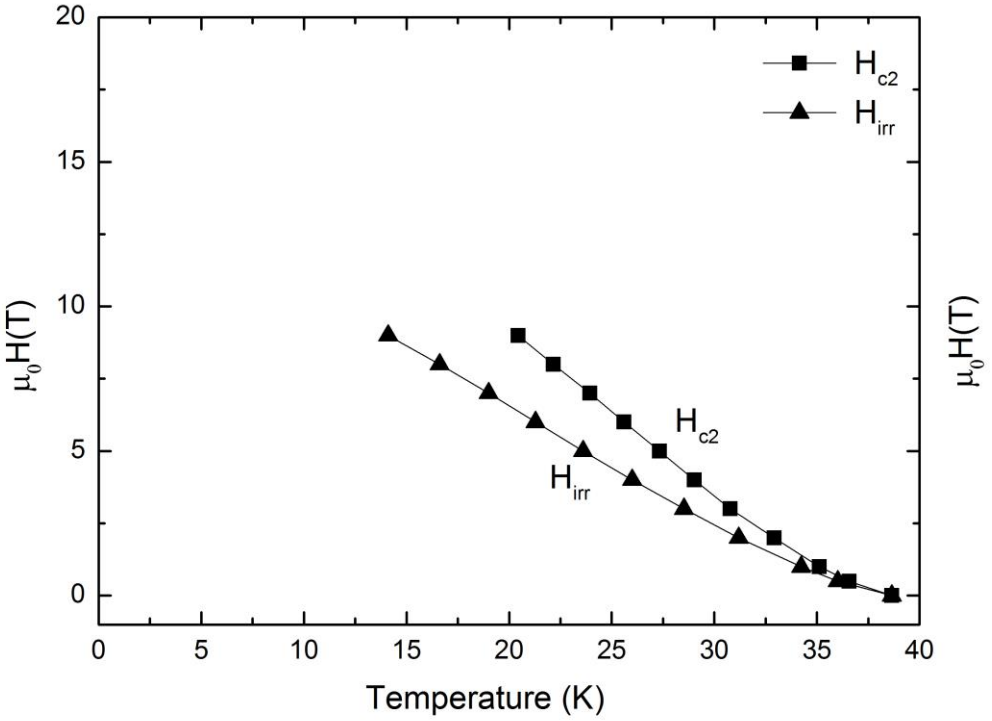

Fig. 7. Dependence of H_{c2} and H_{irr} of infiltrated bulk MgB_2 with temperature. Values estimated using 90%-10% of the normal-state resistivity.